

Cyclops: Open Platform for Scale Truck Platooning

Hyeongyu Lee¹, Jaegeun Park², Changjin Koo¹, Jong-Chan Kim¹, and Yongsoon Eun²

Abstract—Cyclops, introduced in this paper, is an open research platform for everyone that wants to validate novel ideas and approaches in the area of self-driving heavy-duty vehicle platooning. The platform consists of multiple 1/14 scale semi-trailer trucks, a scale proving ground, and associated computing, communication and control modules that enable self-driving on the proving ground. A perception system for each vehicle is composed of a lidar-based object tracking system and a lane detection/control system. The former is to maintain the gap to the leading vehicle and the latter is to maintain the vehicle within the lane by steering control. The lane detection system is optimized for truck platooning where the field of view of the front-facing camera is severely limited due to a small gap to the leading vehicle. This platform is particularly amenable to validate mitigation strategies for safety-critical situations. Indeed, a simplex structure is adopted in the embedded module for testing various fail safe operations. We illustrate a scenario where camera sensor fails in the perception system but the vehicle operates at a reduced capacity to a graceful stop. Details of the Cyclops including 3D CAD designs and algorithm source codes are released for those who want to build similar testbeds.

I. INTRODUCTION

Vehicle platooning is an automation technology that coordinates multiple vehicles so that short longitudinal inter-vehicle distances are maintained while vehicles are running at a high speed [1]. The *leading vehicle* (LV) is usually driven by a human driver, while the *following vehicles* (FVs) are autonomous based on perception sensors and wireless communications between vehicles [2]. Its potential benefits include (i) reduced fuel consumption and emission, (ii) better road utilization, and (iii) enhanced safety [3] [4].

There have been many national-level projects for vehicle platooning, including SARTRE [5] [6] and ENSEMBLE [7] in EU, and TROOP [8] in Korea. We are partly engaged in one of such projects that develops safety scenarios for heavy-duty truck platooning, where the developed system should be validated with potentially fatal scenarios on public highways. The scenarios include (i) emergency braking, (ii) cutting-in rogue vehicles, and (iii) loss of wireless connections. Due to the heavy weights of the employed semi-trailer trucks, we found that it is much too dangerous to put full-size trucks directly into such scenarios in early validation stages. Although Hardware-in-the-Loop (HiL) simulators are employed, they are mostly for validating control algorithms, not for validating countermeasures for safety critical scenarios.

¹Hyeongyu Lee, Changjin Koo are graduate students and Jong-Chan Kim is a professor at the Graduate School of Automotive Engineering, Kookmin University, Seoul, Republic of Korea {a2020011, cj_koo96, jongchank}@kookmin.ac.kr.

²Jaegeun Park is a graduate student and Yongsoon Eun is a professor at the Department of Information and Communication Engineering, DGIST, Daegu, Republic of Korea {jaegeun2, yeun}@dgist.ac.kr.



Fig. 1. Scale semi trailer trucks in Cyclops.

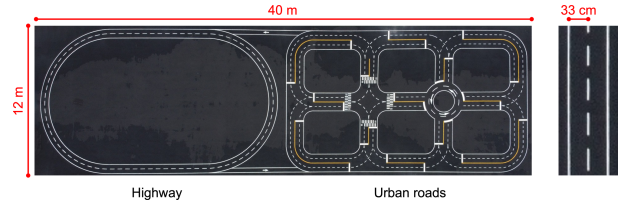


Fig. 2. Scale truck platooning proving ground in Cyclops.

With this motivation, we developed a scale truck platooning testbed, as shown in Fig. 1. We named the testbed as *cyclops* since the front facing single camera on the vehicle reminds us the one-eyed giant in the Greek mythology. Our testbed includes three autonomous semi-trailer trucks, each of which is equipped with perception sensors, computing platforms, and wireless communication devices. With this truck platform, we developed a platooning system with our developed perception and control systems that closely resemble the full-size platooning system. Obviously, it retains most of the real-world challenges for platooning, but significantly reduces the cost of experimenting/validating safety scenarios. It allows us to test and validate safety countermeasures with low cost in the early development stage, even before the full-size trucks are ready. Our platooning system can operate in our scale truck proving ground, as shown in Fig. 2, where various platooning scenarios are rapidly developed and validated.

The perception system on a truck employs one camera sensor and one single-plane lidar sensor. The camera is used for detecting the ego lanes for the lateral control. The lidar is used for measuring the longitudinal distance to and the lateral location of a preceding truck. While developing the perception system, a unique challenge of truck platooning attracted our attention. Since the FVs closely follow the preceding trucks, the rear end of the preceding trailer significantly occludes the camera view, which was also reported in case of full-size trucks [9]. The occlusion adversely affects the lane detection performance because the rear end of the white trailer acts as indistinguishable noise. In order to avoid such situation, our system dynamically determine the Region

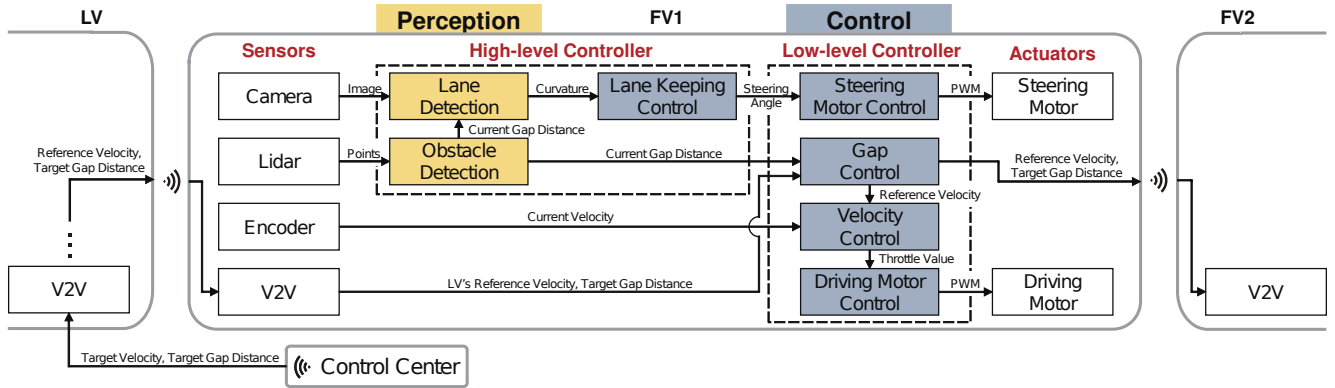


Fig. 3. Cyclops architecture for platooning.

Of Interest (ROI) in the camera image using the distance to the preceding truck: the ROI ends right before the preceding trailer.

For the platooning, the following three control algorithms are developed: (i) velocity control, (ii) gap control, and (iii) lane keeping control. The first is to have the vehicle follow the longitudinal reference velocity. The second is to maintain the distance to the preceding vehicle to a desired gap reference. This control utilizes lidar sensor feedback that measures the distance to the preceding vehicle and the longitudinal reference velocity used in the preceding vehicle through wireless communications. Finally, the third utilizes a camera sensor to locate the vehicle relative to the lanes and adjust steering.

With the developed testbed, we conducted a case study with a camera sensor failure. Since our platooning system relies on the camera for the lateral control, a camera failure surely leads to a catastrophic event. Considering this hazardous safety scenario, we developed a mitigation method that temporarily uses the lidar sensor such that the FV follows the center point of the preceding truck instead of the following the lane, successfully enabling a graceful stop. With this case study, we argue that our testbed can be useful for validating safety algorithms as well as developing various platooning scenarios.

We share in this paper our experience gained while developing the scale truck platooning testbed, and release all the implementation details including the algorithm source codes¹. We hope that our testbed can be reproduced by other research teams that are interested in developing truck platooning systems.

II. TRUCK AND SYSTEM DESIGN

A. System Design

Fig. 3 shows the overall architecture of our platooning system. Three trucks (LV, FV1, and FV2) are connected through a wireless network to each other and with a remote control center. The control center gives the platooning velocity and the target gap distance to the LV, where the

platooning velocity is used as its reference velocity and the target gap distance is communicated to the FV1, which in turn transferred to the FV2. We point out that LV in Cyclops is autonomous while LV in a full-size truck platoon is thought to be human-driven.

In each truck, the perception system receives the front-facing camera images and the lidar data, where the camera image is used for detecting the lane curvature, while the lidar points are used to detect the preceding trailer's rear end. Then the following information is delivered to the control system: (i) the lane curvature, (ii) the distance to the preceding truck, (iii) the current velocity from the encoder sensor, (iv) the target gap distance from the command center, and (v) the preceding truck's reference velocity. In the control system, the lane keeping controller decides the steering angle, which in turn controls the steering motor through the steering motor controller. The gap controller generates the reference velocity to meet the target gap, which is given to the velocity controller that controls the driving motor through the driving motor controller. The reference velocity generated by the gap controller is communicated to the following truck for its own gap control.

Although the LV and the FVs share the same hardware and software architecture, there is a slight difference between them. Since the LV does not have to do the gap control, it instead has the emergency braking controller between the obstacle detection and the velocity controller. Since our testbed allows no other surrounding vehicles at this moment, in case the LV detects an obstacle within its detection range, it automatically enforces an emergency stop, which in turn triggers emergency stops in FV1 and FV2, by setting the LV's reference velocity to zero. Except that, the LV and the FVs are identical. Also note that the command center can also enforce an emergency stop by a remote command.

B. Truck Design

Fig. 4 shows one of our 1/14 scale semi-trailer trucks. As the truck body, we use an RC truck that is famous within the RC enthusiasts. Three such trucks were developed, one of which is designated as an LV, and the others are FVs. In the figure, important components such as the sensors

¹All the design materials and the source codes are available at https://github.com/hyeongyu-lee/scale_truck_control.

TABLE I
SUMMARY OF TRUCK COMPONENTS.

Component	Item
Tractor	1/14 MAN 26.540 6x4 XLX
Trailer	40-Foot Container 1/14 Semi-trailer
Camera	ELP-USBFHD04H-BL180
Lidar	RPLidar A3
Encoder	Magnetic Encoder Pair Kit
High-level controller	Nvidia Jetson AGX Xavier
Low-level controller	OpenCR 1.0
Driving Motor	TBLM-02S 21.5T
Steering motor	SANWA SRM-102
Battery	BiXPower 96Wh BP90-CS10
Antenna	ipTIME N007

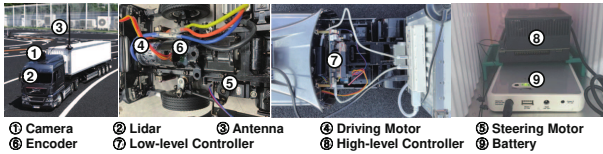


Fig. 4. Scale truck design.

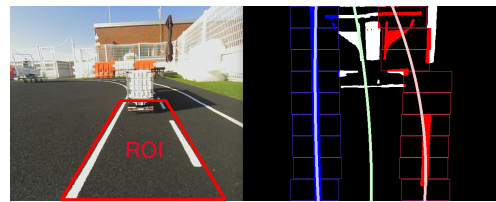
and the computing platforms are located. All three trucks are equipped with the same hardware components listed in Table I. More specifically, each truck is equipped with a 180 degrees FoV (Field of View) front-facing camera on top of the tractor. A single plane lidar sensor with its detection range of 25 m is hidden inside the truck cabin. An encoder that counts the wheel speed is installed at the front wheel of the tractor. As computing platforms, we use two computers, each of which is responsible for the high-level control and the low-level control, respectively. For the high-level controller, we use an Nvidia Jetson AGX Xavier hidden inside the trailer. For the low-level controller, an OpenCR computer is attached at the back of the tractor. For the driving motor, we use a 1800 KV BLDC motor. For the steering motor, we use a servo motor with its torque of 3.3kg-cm. All the electronic components are powered by a 96 Wh battery hidden in the trailer. For the wireless communication, we use the WIFI network in the Nvidia Jetson AGX Xavier. To reinforce the wireless communication, an additional high performance antenna is attached on top of the trailer.

III. PERCEPTION AND CONTROL

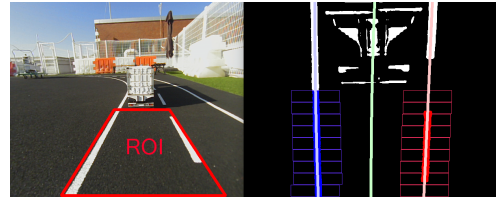
This section presents our perception and control methods for truck platooning. Our platooning system has two different modes of operations (i.e., the LV mode and the FV mode). We implicitly assume the FV mode in this section, and it will be explicitly stated when the LV mode needs to be presented.

A. Lane Detection

The objective of lane detection is to find the curvature of the desired path from the front-facing camera. For that, a camera image goes through the following steps: (i) pre-processing that cuts the trapezoid ROI and removes noise using the Gaussian blur method; (ii) conversion into a binarized bird's eye view image; (iii) sliding window-based search to detect the left and right lanes; (iv) fitting the desired



(a) 0.8 m gap with static ROI.



(b) 0.8 m gap with dynamic ROI.

Fig. 5. Lane detection performance with/without dynamic ROI in a small (0.8m) inter-vehicle gap situation.

path's curvature combining the left and right lane curvatures. The final curvature is decided as a second-order polynomial.

The above lane detection method has been widely used in many studies [10], [11], [12] because it is robust and lightweight for the implementation in small embedded systems. Unfortunately, however, the method does not work well in the platooning scenario due to the excessively small gap to the preceding truck. Fig. 5(a) shows a forward view image and its lane detection result using the static ROI method where the trapezoid ROI is a fixed one. The binary image shows that the slight inclusion of the trailer's rear end in the ROI badly affects the lane detection result. This is an existing issue with full size trucks [9]. In our testbed, the effect is vibrant because the trailer's color happens to be white.

To eliminate the noise by the trailer at a close distance, we try to cut off the trailer portion in the bird's eye view image. For that, we use the gap information from the lidar sensor. By actual measurements, we found that the ratio between the longitudinal distance and the number of vertical pixels is 490 pixels per 1.0 m. With this mapping, Fig. 5(b) shows the adapted ROI that precisely removes the noise, which provides a significantly improved lane detection result. This adaptation logic is added in our lane detection module such that it can dynamically determine the optimal ROI.

B. Obstacle Detection

Obstacle detection provides the gap distance to the preceding truck. We use a single plane lidar sensor that provides a set of points to the nearest objects around 360 degrees. To detect the preceding truck, we limitedly use the front-facing 60 degrees. For the obstacle detection, we employ the well-known obstacle_detector ROS package [13], which detects and also tracks nearby objects by clustering the 2D lidar points. The tracking result is obtained as a circle where its center and diameter correspond to the middle point and the horizontal length of the preceding trailer's rear end, respectively.

C. Velocity Control

In this section, we introduce the velocity control, which consists of feed-forward plus anti-windup proportional-integral (FF+AWPI) control, the velocity saturation function $\text{sat}_i(u_{v,c,i})$, and the inverse of the nonlinear function $f_i^{-1}(\bar{u}_{v,c,i})$. Here, the subscript $i = 0$ denotes the variables or function for the LV, $i = 1$ for the FV1, and $i = 2$ for the FV2. FF+AWPI control calculates velocity control input $u_{v,c,i}$ such that

$$u_{v,c,i}(k) = K_{F,i}v_{r,i}(k) + K_{P,i}\tilde{v}_i(k) + \sum_{j=0}^{j=k} K_{I,i}\tilde{v}_i(j)T_s + \sum_{j=0}^{j=k-1} K_{A,i}(\bar{u}_{v,c,i}(j) - u_{v,c,i}(j)), \quad (1)$$

where T_s is sampling time, $\bar{u}_{v,c,i}$ is the velocity control input saturated by function $\text{sat}_i(u_{v,c,i})$, the positive constants $K_{P,i}$, $K_{F,i}$, $K_{I,i}$, and $K_{A,i}$ are control parameters, and $\bar{v}_{r,i}$ is the saturated velocity reference. The velocity tracking error \tilde{v}_i is given as

$$\tilde{v}_i(k) = \bar{v}_{r,i}(k) - v_i(k), \quad (2)$$

where v_i is velocity measurements of the truck.

The saturation function $\text{sat}_i(u_{v,c,i})$ represents the velocity limitation that a truck can generate. The saturation function $\text{sat}_i(u_{v,c,i})$ is given as

$$\text{sat}_i(u_{v,c,i}) = \begin{cases} V_i^{\max}, & \text{if } u_{v,c,i} \geq V_i^{\max} \\ 0, & \text{if } u_{v,c,i} \leq 0 \\ u_{v,c,i}, & \text{otherwise} \end{cases}, \quad (3)$$

where V_i^{\max} denotes the maximum velocity that a truck can generate.

The motor command and the velocity of the truck have the nonlinear relation. The inverse of nonlinear function $f_i^{-1}(\bar{u}_{v,c,i})$ is used for linearly treating the truck. The nonlinear function $f_i(u_i)$ representing the nonlinearity between the motor command and the velocity of the truck is obtained by fitting the experimental data for the motor command and the velocity of truck into quadratic function, and is given by

$$f_i(u_i) = a_i u_i^2 + b_i u_i + c_i, \quad (4)$$

where a_i , b_i , and c_i are design parameters. From (4), we can induce the function $f_i^{-1}(\bar{u}_{v,c,i})$ such that

$$f_i^{-1}(\bar{u}_{v,c,i}) = \frac{-b_i + \sqrt{b_i^2 - 4a_i(c_i - \bar{u}_{v,c,i})}}{2a_i}. \quad (5)$$

Finally, the output of the function $f_i^{-1}(\bar{u}_{v,c,i})$ is the motor command u_i , which is applied to driving motor.

D. Gap Control

The gap control is used by only FVs. The goal of gap control is to make the gap to the preceding truck into the gap reference. The gap control is composed of the feed-forward plus proportional-differential (FF+PD) control and

the velocity reference saturation function $\text{sat}_{r,i}(v_{r,i})$. The FF+PD control is given in the following form:

$$v_{r,i}(k) = \bar{v}_{r,i-1}(k) - K_{GP,i}\tilde{d}_i(k) - \frac{K_{GD,i}(\tilde{d}_i(k) - \tilde{d}_i(k-1))}{T_s}, \quad (6)$$

where $\bar{v}_{r,i-1}$ is the saturated velocity reference of preceding truck received via wireless communication. The positive constants $K_{GP,i}$ and $K_{GD,i}$ are control parameters, and the gap tracking error \tilde{d}_i is obtained as

$$\tilde{d}_i(k) = d_{r,i}(k) - d_i(k), \quad (7)$$

where $d_{r,i}$ denotes the gap reference and d_i denotes the measured gap to the preceding truck.

The velocity reference saturation function $\text{sat}_{r,i}(v_{r,i})$ saturates the velocity reference as the velocity limit of the lane, which is represented as

$$\text{sat}_i(v_{r,i}) = \begin{cases} V_r^{\max}, & \text{if } v_{r,i} \geq V_r^{\max} \\ 0, & \text{if } v_{r,i} \leq 0 \\ v_{r,i}, & \text{otherwise} \end{cases}, \quad (8)$$

where V_r^{\max} denotes the velocity limit of the lane. Finally, the saturated velocity reference $\bar{v}_{r,i}$ plays the role of velocity reference for velocity control.

E. Lane Keeping Control

In this section, we introduce lane keeping control to maintain the truck within the lane. The lane keeping control is given by

$$\delta_i(k) = -K_i(v_i)e_i(k) - K_{L,i}(v_i)e_{L,i}(k), \quad (9)$$

where δ_i is steering angle, e_i is the estimated lateral error, $e_{L,i}$ is preview lateral error, and $K_i(v_i)$ and $K_{L,i}(v_i)$ are control parameters that are varied according to truck velocity. Because the faster the velocity is, the bigger the change in lateral position by the steering angle, if the velocity is faster, the control parameters have to be smaller.

In (9), the preview lateral error $e_{L,i}$ is obtained with a camera sensor. The lateral error e_i , however, cannot be directly obtained with a camera sensor due to the limited sight of a camera sensor, thus we estimate the lateral error e_i such that

$$e_i(k) = e_{L,i}(k) - L_i \tan(\theta_i(k)), \quad (10)$$

where L_i is the preview distance and θ_i is the angle between the direction in which the truck moves and the preview point on the desired path which is obtained with a camera sensor.

IV. EXPERIMENTS

In this section, we illustrate the performance of platooning with the three trucks in our proving ground in Fig. 2, by conducting two experimental scenarios. The first scenario is to speed up the LV while maintaining the constant gap between trucks, and the other scenario is to reducing the gap between trucks while maintaining the constant velocity

TABLE II
PARAMETERS FOR NONLINEAR FUNCTION.

i	a_i	b_i	c_i
0	-1.1446×10^{-5}	0.048278	-47.94
1	-2.0975×10^{-5}	0.08152	-76.87
2	-1.0444×10^{-5}	0.043253	-42.3682

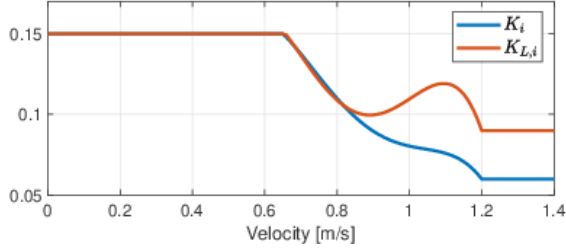


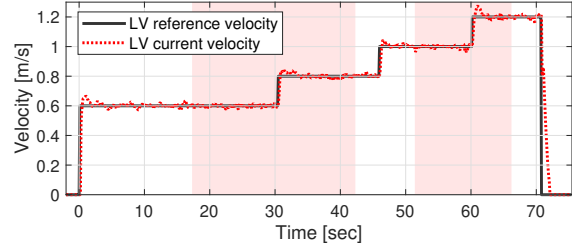
Fig. 6. Lane keeping control parameters in the experiments.

of the LV. We also evaluate the effectiveness of the dynamic ROI via the experiments. As mentioned in previous section, a camera sensor cannot measure the lateral error, but the lateral error is required to validate the performance of the lane keeping control. Thus, we install a extra camera sensor at the side of each trailer of all the trucks to measure the lateral error. In the experiments, velocity control parameters of all the trucks in (1) are identically chosen as $K_{F,i} = 1$, $K_{P,i} = 0.8$, $K_{I,i} = 2.0$, and $K_{A,i} = 0.0001$ for $i = 0, 1, 2$. The parameters a_i, b_i and c_i in (4) are selected as Table II. Gap control parameters of FV1 and FV2 in (6) are also identically chosen as $K_{GP,i} = 0.5$ and $K_{GD,i} = 0.1$ for $i = 1, 2$. Lane keeping control parameters of all the trucks are designed as shown in Fig. 6. The parameter V_i^{\max} for $i = 0, 1, 2$ in (3) is selected as 2 m/s and V_r^{\max} in (8) is chosen as 1.4 m/s. In the following graphs, the red colored areas commonly indicate that the LV is in the curved road segments.

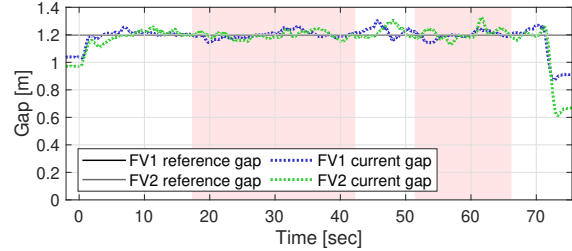
A. Performance of Platooning with Three Trucks

Fig. 7 and Fig. 8 show the experimental results for two scenarios, respectively, for validating the performance of platooning with three trucks. As shown in Fig. 7(a) and Fig. 7(b), all the trucks maintain the desired gap well although the LV speeds up. The lateral errors, meanwhile, increase when the velocity of the LV is bigger than about 1 m/s, but all the trucks maintain within the lane. As a result, the platooning can be performed well up to the velocity of 1.2 m/s.

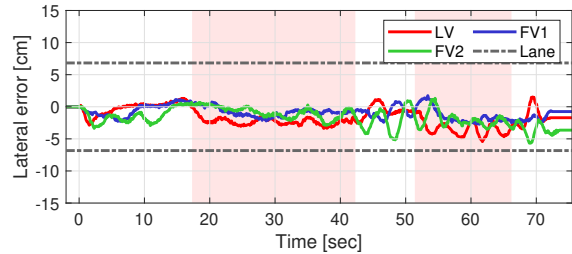
In Fig. 8, we can confirm that FV1 and FV2 reduce the gap to the preceding truck to each gap reference while the LV runs as fast as 1 m/s and all the trucks maintain within the lane. Therefore, it is validated that three trucks can change the gap between trucks on the move. However, in Fig. 8(b) and Fig. 8(c), we can see that the lateral error is getting bigger when the gap between trucks is as small as 0.6 m. As mentioned before, this phenomena occurs when the gap is too short such that the camera's views is significantly occluded by the preceding truck. In order to solve this problem, we



(a) Velocity control performance.



(b) Gap control performance.



(c) Lane keeping control performance.

Fig. 7. Experimental result platooning performance in Scenario 1.

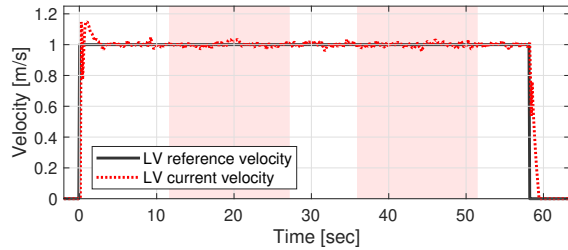
apply the dynamic ROI method to the lane detection and the experimental result of it appears in the next section.

B. Effectiveness of Dynamic ROI

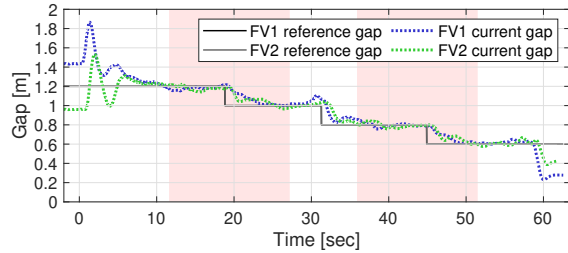
Fig. 9 shows the lateral error of FV2 when using the static ROI and when using the dynamic ROI, respectively. In this experiment, FV2 maintains the gap to the FV1 at 0.6 m. As shown in Fig. 9, the size of the lateral error when applying the dynamic ROI is smaller than the size of the lateral error when applying the static ROI. The FV2, besides, goes out the lane at about 51.4 seconds when applying the static ROI. Therefore, we can conclude that the dynamic ROI is effective in lane detection when the gap between trucks is too short such that the camera's view is significantly occluded by the preceding truck.

V. CASE STUDY: CAMERA SENSOR FAILURE

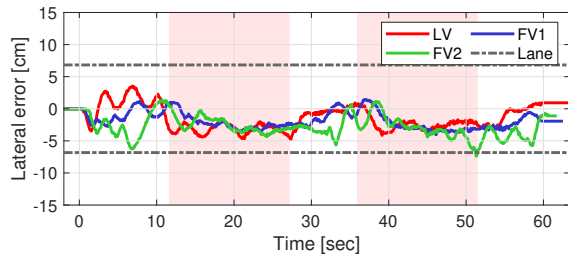
To show how our testbed can be helpful in developing safety scenarios, we conducted a case study, that is, developing a mitigation method for a camera sensor failure scenario on our testbed. Since the lateral control purely depends on the camera sensor, its failure can be a catastrophic event. In such a fatal scenario, one possible method is to use the remaining lidar sensor to follow the preceding trailer's center,



(a) Velocity control performance.



(b) Gap control performance.



(c) Lane keeping control performance.

Fig. 8. Experimental result platooning performance in Scenario 2.

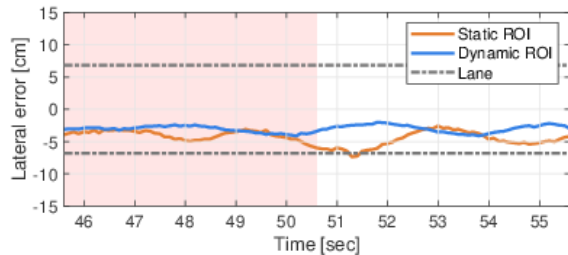


Fig. 9. Lane keeping performance with/without using dynamic ROI in camera image processing.

even without knowing the lane curvature. By this method, the platoon can buy enough time until it slowly stops while maintaining minimal safety.

For the experiment, we implemented a fault injection scenario that simulates a cut wire from the camera in the FV1. In such cases, the old image is repeatedly fed into the perception system such that the failure can be detected by comparing the current image with old images assuming that the truck's velocity is not zero. Then the truck goes into a fail-safe mode that no longer uses the lane detection result and follows the preceding truck's center. The failure is also notified to the LV such that the entire platoon goes into a

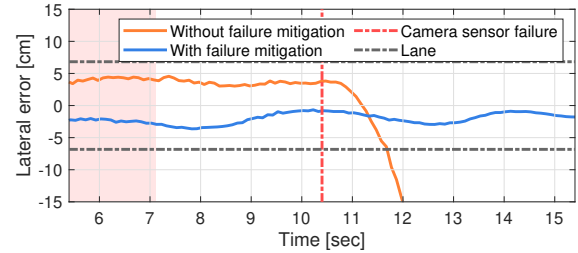


Fig. 10. Lane keeping performance with/without the camera failure mitigation method.

fail-safe mode, slowing down until a graceful stop.

Fig. 10 compares the FV1's lateral error for two scenarios. One is without any failure mitigation method, and the other is with our failure mitigation method. For the measurement, the platoon drives at a velocity of 0.8 m/s with a gap of 0.8 m. After the LV reaches a straight road segment, a fault is injected into the FV1's camera. The figure shows that the truck quickly goes out of the lane without the mitigation method, whereas our mitigation method makes it keep its lane even though the lateral oscillation is slightly amplified.

VI. RELATED WORLD

The truck platooning technology has been developed through national flagship projects [1], [3], [5], [6], [14], [15], [16]. Most studies thus far have dealt with control issues [17], [18], [19], [20], fuel economy [21], [22], [23], and safety issues [24], [25], [26]. To the best of our knowledge, our study is one of the first attempts to implement a scale truck platooning tested.

VII. CONCLUSION

We presented Cyclops, a scale truck platooning testbed, targeting an open research platform for everyone interested in the truck platooning technology. Our platooning system uses wireless communications as well as camera and lidar sensors to maintain a constant gap at a given platooning velocity. We implemented our perception and control systems optimized for solving the platooning system's unique challenges caused by the excessively small gaps. With our scale trucks, we successfully validated the control stability up to 1.2 m/s, corresponding to about 60 km/h in real trucks. Also, we can safely reduce the gap until it reaches 0.6 m, which corresponds to 8.4 m in real trucks, at the velocity of 1.0 m/s. Furthermore, on top of the platooning system, we conducted a case study that validates a camera failure mitigation method that is difficult to realize with real trucks due to its high risks. We hope our testbed can benefit many researchers by releasing all the details of our work on Github.

REFERENCES

- [1] C. Bergenheim, S. Shladover, E. Coelingh, C. Englund, and S. Tsugawa, "Overview of platooning systems," in *Proceedings of the 19th ITS World Congress, Oct 22-26, Vienna, Austria (2012)*, 2012.
- [2] C. Bergenheim, E. Hedin, and D. Skarin, "Vehicle-to-vehicle communication for a platooning system," *Procedia-Social and Behavioral Sciences*, vol. 48, pp. 1222–1233, 2012.

- [3] S. Tsugawa, S. Jeschke, and S. E. Shladover, "A review of truck platooning projects for energy savings," *IEEE Transactions on Intelligent Vehicles*, vol. 1, no. 1, pp. 68–77, 2016.
- [4] J. Lioris, R. Pedarsani, F. Y. Tascikaraoglu, and P. Varaiya, "Doubling throughput in urban roads by platooning," *IFAC-PapersOnLine*, vol. 49, no. 3, pp. 49–54, 2016.
- [5] T. Robinson, E. Chan, and E. Coelingh, "Operating platoons on public motorways: An introduction to the sarthe platooning programme," in *17th world congress on intelligent transport systems*, vol. 1, 2010, p. 12.
- [6] C. Berghem, Q. Huang, A. Benmimoun, and T. Robinson, "Challenges of platooning on public motorways," in *17th world congress on intelligent transport systems*, 2010, pp. 1–12.
- [7] L. Konstantinopoulou, A. Coda, and F. Schmidt, "Specifications for Multi-Brand Truck Platooning," in *ICWIM8, 8th International Conference on Weigh-In-Motion*, 2019, pp. 8–p.
- [8] Y. Lee, T. Ahn, C. Lee, S. Kim, and K. Park, "A novel path planning algorithm for truck platooning using v2v communication," *Sensors*, vol. 20, no. 24, p. 7022, 2020.
- [9] T.-W. Kim, W.-S. Jang, J. Jang, and J.-C. Kim, "Camera and radar-based perception system for truck platooning," in *2020 20th International Conference on Control, Automation and Systems (ICCAS)*. IEEE, 2020, pp. 950–955.
- [10] Y. Fan, W. Zhang, X. Li, L. Zhang, and Z. Cheng, "A robust lane boundaries detection algorithm based on gradient distribution features," in *2011 Eighth International Conference on Fuzzy Systems and Knowledge Discovery (FSKD)*, vol. 3. IEEE, 2011, pp. 1714–1718.
- [11] X. Zhang, M. Chen, and X. Zhan, "A combined approach to single-camera-based lane detection in driverless navigation," in *2018 IEEE/ION Position, Location and Navigation Symposium (PLANS)*. IEEE, 2018, pp. 1042–1046.
- [12] M. R. Haque, M. M. Islam, K. S. Alam, H. Iqbal, and M. E. Shaik, "A computer vision based lane detection approach," *International Journal of Image, Graphics and Signal Processing*, vol. 12, no. 3, p. 27, 2019.
- [13] M. Przybyla, "obstacle_detector," https://github.com/tysik/obstacle_detector, 2018.
- [14] S. Tsugawa, S. Kato, and K. Aoki, "An automated truck platoon for energy saving," in *2011 IEEE/RSJ International Conference on Intelligent Robots and Systems*. IEEE, 2011, pp. 4109–4114.
- [23] A. Al Alam, A. Gattami, and K. H. Johansson, "An experimental study on the fuel reduction potential of heavy duty vehicle platooning," in *13th International IEEE Conference on Intelligent Transportation Systems*. IEEE, 2010, pp. 306–311.
- [15] J. B. Michael, D. N. Godbole, J. Lygeros, and R. Sengupta, "Capacity analysis of traffic flow over a single-lane automated highway system," *Journal of Intelligent Transportation System*, vol. 4, no. 1-2, pp. 49–80, 1998.
- [16] J. Carbaugh, D. N. Godbole, and R. Sengupta, "Safety and capacity analysis of automated and manual highway systems," *Transportation Research Part C: Emerging Technologies*, vol. 6, no. 1-2, pp. 69–99, 1998.
- [17] R. Rajamani, H.-S. Tan, B. K. Law, and W.-B. Zhang, "Demonstration of integrated longitudinal and lateral control for the operation of automated vehicles in platoons," *IEEE Transactions on Control Systems Technology*, vol. 8, no. 4, pp. 695–708, 2000.
- [18] J. Ploeg, D. P. Shukla, N. van de Wouw, and H. Nijmeijer, "Controller synthesis for string stability of vehicle platoons," *IEEE Transactions on Intelligent Transportation Systems*, vol. 15, no. 2, pp. 854–865, 2013.
- [19] A. Alam, J. Mårtensson, and K. H. Johansson, "Experimental evaluation of decentralized cooperative cruise control for heavy-duty vehicle platooning," *Control Engineering Practice*, vol. 38, pp. 11–25, 2015.
- [20] B. Besselink and K. H. Johansson, "String stability and a delay-based spacing policy for vehicle platoons subject to disturbances," *IEEE Transactions on Automatic Control*, vol. 62, no. 9, pp. 4376–4391, 2017.
- [21] A. Alam, B. Besselink, V. Turri, J. Martensson, and K. H. Johansson, "Heavy-duty vehicle platooning for sustainable freight transportation: A cooperative method to enhance safety and efficiency," *IEEE Control Systems Magazine*, vol. 35, no. 6, pp. 34–56, 2015.
- [22] V. Turri, B. Besselink, and K. H. Johansson, "Cooperative look-ahead control for fuel-efficient and safe heavy-duty vehicle platooning," *IEEE Transactions on Control Systems Technology*, vol. 25, no. 1, pp. 12–28, 2016.
- [24] E. van Nunen, D. Tzempetzis, G. Koudijs, H. Nijmeijer, and M. van den Brand, "Towards a safety mechanism for platooning," in *2016 IEEE Intelligent Vehicles Symposium (IV)*. IEEE, 2016, pp. 502–507.
- [25] T. Bijlsma and T. Hendriks, "A fail-operational truck platooning architecture," in *2017 IEEE Intelligent Vehicles Symposium (IV)*. IEEE, 2017, pp. 1819–1826.
- [26] E. van Nunen, F. Esposto, A. K. Saberi, and J.-P. Paardekooper, "Evaluation of safety indicators for truck platooning," in *2017 IEEE Intelligent Vehicles Symposium (IV)*. IEEE, 2017, pp. 1013–1018.